

Integrated Dynamic Analysis of Floating Offshore Wind Turbines

Finn Gunnar Nielsen, Tor David Hanson, Bjørn Skaare

Hydro Oil & Energy, P.O. Box 7190, N – 5020 Bergen, Norway, tel. +47 55 99 50 00, fax. +47 55996928
Finn.Gunnar.Nielsen@hydro.com, Tor.David.Hanson@hydro.no, Bjorn.Skaare@hydro.no

Summary

Two different simulation models for integrated dynamic analysis of floating offshore wind turbines are described and compared with model scale experiments for the Hywind concept for floating offshore wind turbines.

A variety of both environmental conditions and wind turbine control schemes are tested. A maximum power control strategy is applied for wind velocities below the rated wind speed for the wind turbine, while a constant power control strategy is achieved by controlling the rotor blade pitch angle for wind velocities above rated wind speed.

Conventional rotor blade pitch control for wind velocities above rated wind speed introduces negative damping of the tower motion. This results in excitation of the natural frequency in pitch for the tower and may lead to unacceptable tower motions. Active damping of the undesirable tower motions is obtained by using an additional pitch control algorithm based on measurement of the tower velocity.

1. Introduction

The development of wind power technology has resulted in large wind turbines that have so far only been installed on land and in shallow waters offshore. Wind turbines at sea are a good solution because they will not interfere with life on land. In addition to steadier breezes and higher annual mean wind velocity, one can achieve better energy efficiency at sea than on land. Presently, offshore wind turbines are installed in shallow waters on piled or gravity-based foundations. See e.g. Middelgrunden Offshore Wind Farm [1]. Such fixed foundation can be used without major problems in water depth up to approximately 20 m. For larger water depth problems with the natural periods of the system is likely. Also the installation of the tower and turbine becomes more complicated. For water depth between approximately 20m and 60m various tripod and quadropod solutions have been proposed, e.g. the OWEC tower at the Beatrice Windfarm, [2]. For deeper waters floating foundations may be an attractive solution. Various floating foundations for structures that should float in water depth of about 50 m are studied in [3] and [4]. The main challenges are to combine stability, acceptable motions and low costs. A study in [5] concluded that a three-leg tension leg support structure was the most promising solution. However it has been considered too expensive. Floating concepts for deeper water are studied in [6] and [7], which also focus on the cost challenge, but conclude that deep water floating support structure should be viable if multiple unit series production and value engineering is considered.

If we consider water depth above 100m and accept a deep draft hull it is easier to find attractive solutions for floating foundations. A slender deep draft hull make static stability requirements easy to fulfil, the wave loads are moderate on a deep slender structure, efficient low cost production is possible and not at least: All construction work may be performed in sheltered waters. The complete structure can thus be towed to its permanent location where the only offshore marine operations to be performed are hook up of mooring lines and electrical cable.

Hywind, Figure 1 is Norsk Hydro's proposal for such a deep-water floating wind turbine. The hull is to be produced in concrete. On top of the concrete section a steel tower is mounted. The hull is moored by three lines consisting of steel wires and clump weights. The present version is designed for a 5 MW turbine. The key parameters for the concept are given in Table 1. The system consists thus of well proven offshore components. The electrical power generated by the wind turbine will be transported by cable to shore or to offshore oil and gas installations.

A key issue in the development of the Hywind concept has been to predict the dynamic behaviour of the system. In the following, two approaches used will be described together with some sample results.

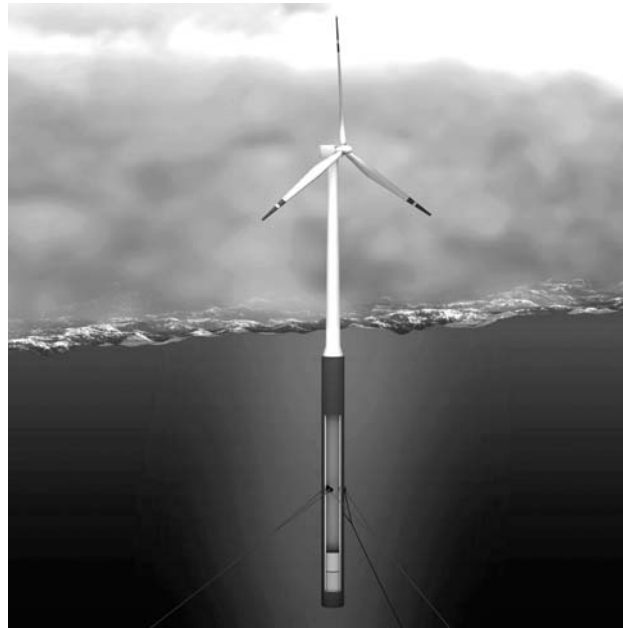


Figure 1. The Hywind floating wind turbine concept.

Turbine power	5MW
Nacelle height above water line	81.5m
Rotor diameter	123m
Water depth	200 – 700m
Displacement	7950 m ³
Mooring	3 lines

Table 1. Main particulars for the 5 MW Hywind concept.

2. Dynamics of Floating Wind Turbines

The dynamic models for the to different simulation programs for a floating wind turbine, HywindSim and Simo-Riflex, are presented in this section. Simo-Riflex is the coupled mode of the Marintek programs Simo and Riflex, and is state of art code for analysis of coupled rigid and/or flexible floating bodies. HywindSim is an in-house MATLAB/Simulink code that is developed in order to have a simple and transparent code for comparison with more advanced codes.

Hydrodynamic Model for HywindSim

The implemented hydrodynamic model is based upon the following:

Hydrostatic forces as well as added mass and radiation damping are all linearized. I.e. they are computed for the initial equilibrium position of the hull. Added mass and radiation damping were obtained from a linear boundary element radiation diffraction program (WAMIT, [8]). For the actual hull parameters added mass could be considered frequency independent and radiation damping could be neglected.

The wave excitation forces were computed applying a long wavelength strip theory approach and Morison equation. The variation in diameter along the depth is thus accounted for, see Figure 2. The forces are calculated at the initial position of the body, but the velocity of the body is included in the drag term. A drag term acting at the waterline is included. This term accounts for the relative wave elevation and horizontal velocity in the waves at the free surface.

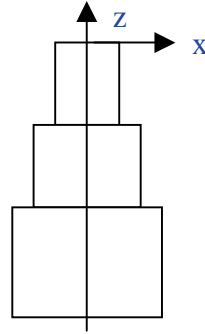


Figure 2. Modelling of a hull with variable diameter.

Hydrodynamic Model for Simo-Riflex

The hydrodynamic model is similar to the HywindSim implementation, but contrary to the HywindSim implementation, the Simo-Riflex implementation computes the hydrodynamic loads at the actually displaced position of the structure and full equilibrium iteration is carried out for each time step. Thereby e.g. vertical forces due to the coupling between transverse forces and the instantaneous pitch angle are accounted for, see e.g. [9].

Mooring Force Model for HywindSim

The mooring force model is based upon a quasi-static formulation that uses interpolation between pre-calculated mooring line forces. The horizontal and the vertical mooring force component are found from input of the horizontal and the vertical mooring line distance to MATLAB/Simulink's 3D look-up tables. The effect of the "crowfoot" on the mooring lines (as seen in Figure 1) is incorporated by calculating the moments due to the mooring forces at the connection point of the "crowfoot".

Mooring Force Model for Simo-Riflex

The mooring system is an integrated part of the total Simo-Riflex dynamic system. Mooring lines are modeled as elastic cable elements including clump-weight and "crowfoot". In this way the yaw-stiffness due to the "crowfoot" as well as the effect of drag forces on the mooring lines are taken care of.

Kinematic Model for HywindSim

The kinematic model of the floating wind turbine consists of three rigid bodies with coupled dynamics:

- The *tower* that moves with six degrees of freedom
- The *nacelle* that is connected to the *tower* and can rotate relative to the *tower*. In addition, the *nacelle* can have a static tilt angle relative to the *tower*.
- The *rotor* that is connected to the *nacelle* and rotates relative to the *nacelle*.

The 18 governing equations of motion for the floating wind turbine are found from the balance of linear momentum and angular momentum for each body. The governing equations of motion can be reduced from 18 to 8 dynamic equations by use of the couplings between the bodies and can be written on the form

$$M(x)\ddot{x} = f(x, \dot{x}) + \lambda, \quad (1)$$

where

- $M \in \mathbb{R}^{8 \times 8}$ is the mass matrix for the system, including the hydrodynamic mass.
- $f \in \mathbb{R}^{8 \times 1}$ is a nonlinear vector function depending on the state and state velocity of the system.
- $\lambda \in \mathbb{R}^{8 \times 1}$ is a vector of external forces.
- $x \in \mathbb{R}^{8 \times 1}$ is the state vector of the system and contains the positions of the tower in the waterline, the Euler angles for the tower (roll-pitch-yaw), the nacelle angle and the rotor angle.

Kinematic Model for Simo-Riflex

The Riflex system is based on a co-rotated Lagrangian formulation that incorporates unlimited translation and rotation in 3D combined with small strain theory for the flexible beam elements. A detailed description of the model is given

in [10]. The tower with nacelle is modeled as one body comprising of approximately 60 flexible linear beam elements each having 12 degrees of freedom. The rotor is a rigid body element rotating with constant velocity. In addition to calculating the rigid body motion of the system this also allows for investigation of the elastic behaviour of the tower including dynamical excitation of the natural bending modes, as well as the rigid-body yaw motions and elastic deflection caused by the gyro-effect of the rotor.

Wind Turbine Model

A simplified wind turbine model is used in the present simulations. Work is ongoing to incorporate a state of art wind turbine model in the simulations. The wind turbine model used in the simulations is identical for the two simulation models and is based on a look-up table for the thrust force coefficient $C_T(U_r)$ for a conventional blade pitch controlled wind turbine. The thrust force F_T on the turbine is based on [11] and is given as

$$F_T = \frac{1}{2} \rho_a A u_{rel}^2 C_T(U_r), \quad (2)$$

where ρ_a is the density of air, A is the total area swept by the rotor and U_r is the relative velocity between the incoming wind and the turbine. The thrust force coefficient depends on the control strategy for the wind turbine. The control strategy for wind velocities below the rated wind speed is to control the rotational speed of the rotor in order to achieve maximum power, while the control strategy above rated wind speed is to achieve constant power. The latter is obtained by rotor blade pitch control. The applied thrust force coefficient $C_T(U_r)$ is shown as function of the relative wind velocity in Figure 3. The blade pitch controller is activated for relative wind velocities above 8.7 m/s, and it is seen that the thrust force coefficient is decreasing with increasing relative wind velocities above rated wind speed. This effect may introduce negative damping in the system that may lead to large resonant motions of the floating wind turbine.

An additional blade pitch control algorithm for active damping of the tower motions, based on measurement of the horizontal tower velocity, has been developed in order to avoid large resonant tower motions above rated wind speed. A simplified active damping control strategy is incorporated in the simulation models by use of a notch filter on the tower velocity signal, tuned to the natural frequency in pitch for the tower, before the thrust force coefficient $C_T(U_r)$ is calculated.

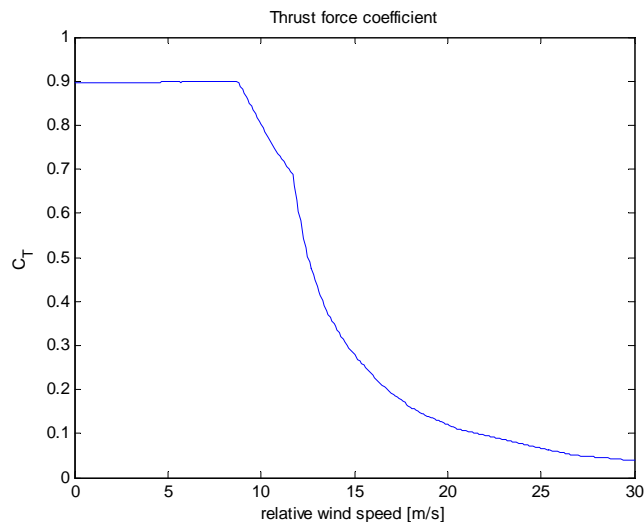


Figure 3: Thrust force coefficient as function of relative wind velocity.

3. Model Scale Experiments

Model scale experiments were carried out at the Ocean Basin Laboratory at Marintek in Trondheim, in order to validate the motion characteristics of the Hywind concept when exposed to coupled wave and wind loads. The basin has dimensions 50m * 80m.

The focus of the model scale experiments were challenging dynamic aspects like:

- Behaviour during a 100 year wave condition
- Behaviour in wind velocities above rated wind speed.
- Behaviour during "average wave conditions" with wind velocities below rated wind speed.

The physical model had a linear scale. 1:47. Froude scaling was applied. The model and the experimental set-up are shown in Figure 4. The following parameters were measured during the experiments:

- Wind velocity
- Wave elevation in front and parallel to the structure.
- Tower motions in six degrees of freedom (6 DOF)
- Mooring line loads.
- Axial acceleration at nacelle level.
- Shear force between nacelle and tower.
- Rotational speed of rotor.

- Blade pitch angle.

Two DC motors were used for control of the rotational speed of the rotor and for the rotor pitch angle. Based on estimates of the relative velocity between the incoming wind and the turbine, the DC motors were controlled in order to incorporate the dynamic behaviour of a real wind turbine, both above and below rated wind speed. The following control schemes were implemented:

- Maximum power production below rated wind speed. Fixed blade pitch, variable rotational speed.
- Constant power above rated wind speed. Fixed rotational speed, variable blade pitch.
- Constant power above rated wind speed with active motion damping. Same as above, but an additional control algorithm to ensure positive motion damping.

A comprehensive test program was carried out with a variety of sea states, wind velocities and control algorithms. In addition “wind only”, “waves only”, motion decay tests etc. were carried out.

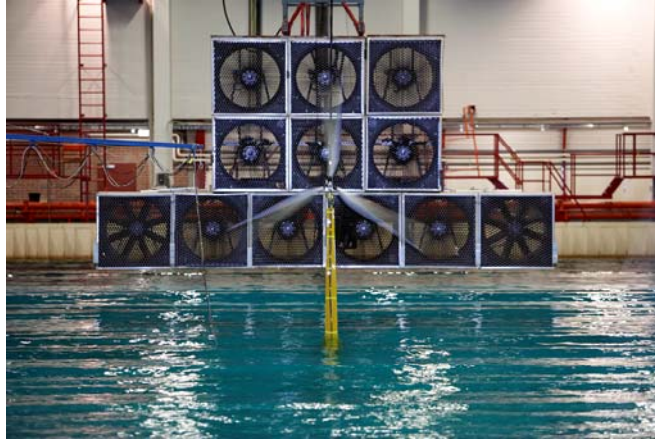


Figure 4. Experimental scale model.

4. Examples of Results

Samples of the results are presented for the following cases

- Average wind speed $U_w = 8$ m/s, JONSWAP wave spectrum with significant wave height $H_s = 3$ m and peak period $T_p = 10$ s. Maximum power control strategy.
- Average wind speed $U_w = 17$ m/s, JONSWAP wave spectrum with significant wave height $H_s = 5$ m and peak period $T_p = 12$ s. Constant power control strategy.
- Average wind speed $U_w = 17$ m/s, JONSWAP wave spectrum with significant wave height $H_s = 5$ m and peak period $T_p = 12$ s. Constant power control strategy + active damping.

A general observation is that the precalculated wave frequency responses are very similar to those measured during the experiments. The challenging part is the resonant motions. Here a significant coupling between aerodynamic loads, wave loads and control algorithm is present.

Wind velocity below rated

In Figure 5 – Figure 7 the square root of the power spectra for the surge motion at the nacelle level is shown for the simulations and the experiments in a case with wind velocity below rated. We observe wave induced motions in the frequency range 0.07 – 0.2 Hz. Below 0.05 Hz two response peaks are present. These are the surge and pitch resonant motions. The pitch response is broad-banded, indicating wind gust excitation and heavy damping. From the above discussion heavy damping should be expected in this case. The computed results from HywindSim and Simo-Riflex are very similar. The experimental results exhibit even less resonant response.

Wind velocity above rated.

The results are presented in Figure 8 – Figure 10. The most characteristic feature of all the figures is the very sharp response peak at resonance. This was expected as the control algorithm adds negative damping to the system. We observe that HywindSim estimates the largest resonant response. This is probably due to the linear force formulation and the lack of mooring line damping. However, also Simo-Riflex overestimates the response. Low damping estimates in the computations as well as transient effects in the lift forces on the turbine blades may contribute to the explanation of this observation. This transient effect, [12] delays the changes in lift forces relative to the change in blade pitch angle or change in incident relative velocity. Note that the Simo-Riflex simulations in Figure 9 and Figure 12 also contain a fourth peak that is due to the first bending mode of the tower.

Above rated wind velocity. Including active damping.

The results are presented in Figure 11 - Figure 13. It is seen from the figures that introduction of the active damping control strategy reduces the resonant pitch motion considerably, both in simulations and experiments. In the experiments the damping algorithm proved so efficient that the resonant pitch motion virtually is removed.

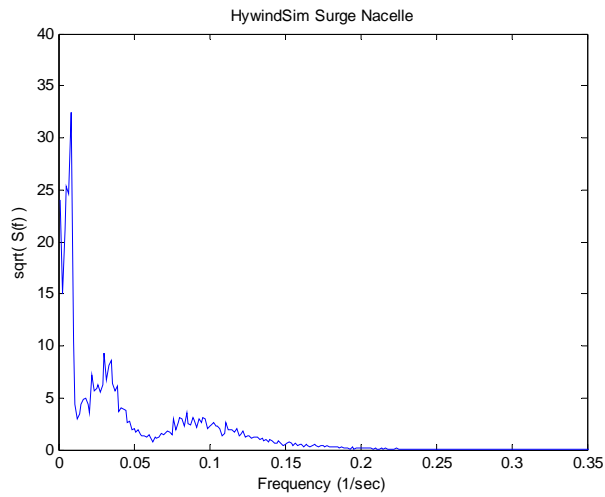


Figure 5. HywindSim simulations. $H_s = 3$ m, $T_p = 10$ s, $U_w = 8$ m/s.

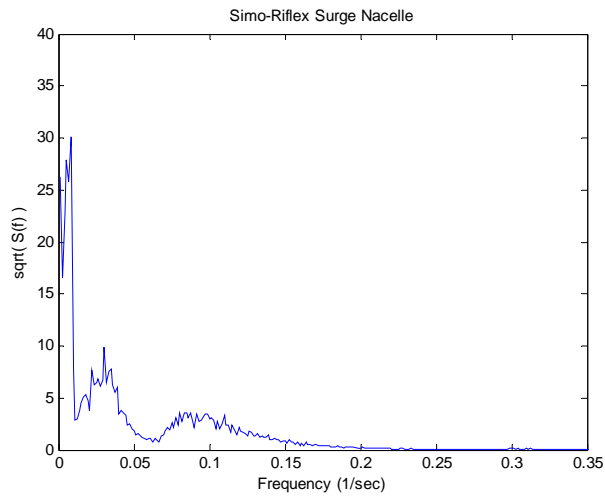


Figure 6. Simo-Riflex simulations. $H_s = 3$ m, $T_p = 10$ s, $U_w = 8$ m/s.

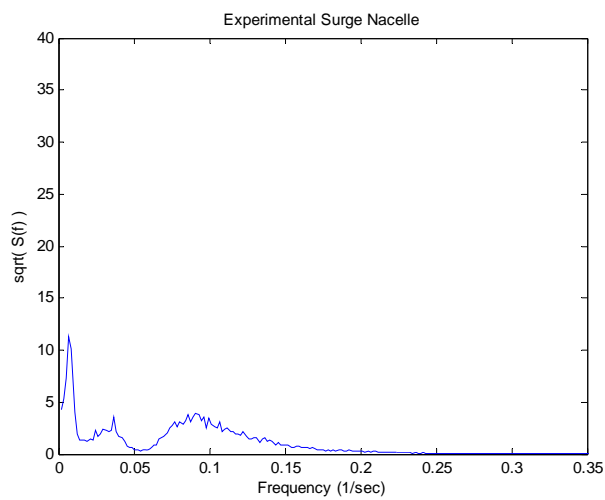


Figure 7. Experimental results. $H_s = 3$ m, $T_p = 10$ s, $U_w = 8$ m/s.

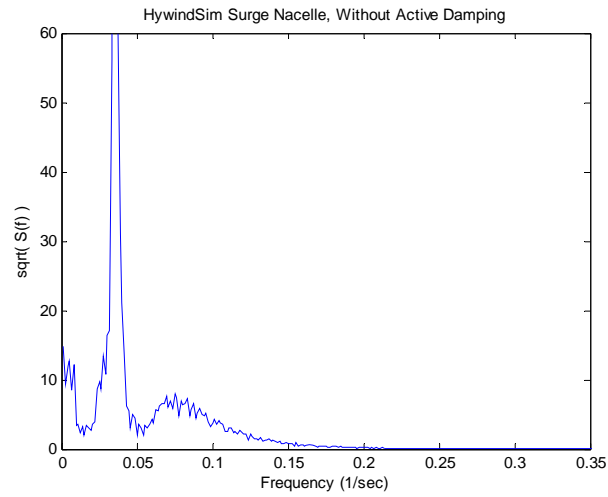


Figure 8. HywindSim simulations without active damping. $H_s = 5\text{m}$, $T_p = 12\text{s}$, $U_w = 17\text{ m/s}$.

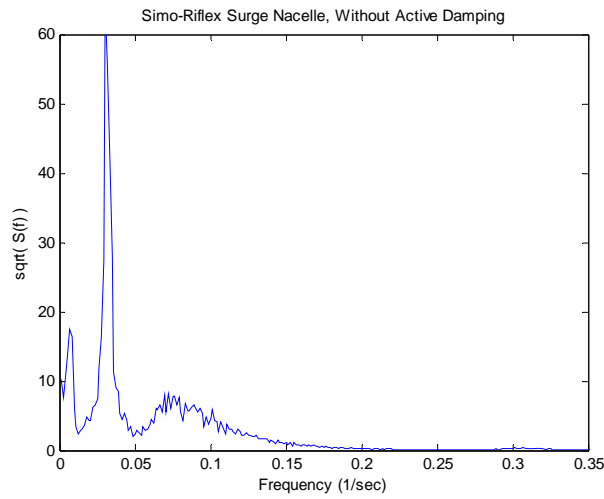


Figure 9. Simo-Riflex simulations without active damping. $H_s = 5\text{m}$, $T_p = 12\text{s}$, $U_w = 17\text{ m/s}$.

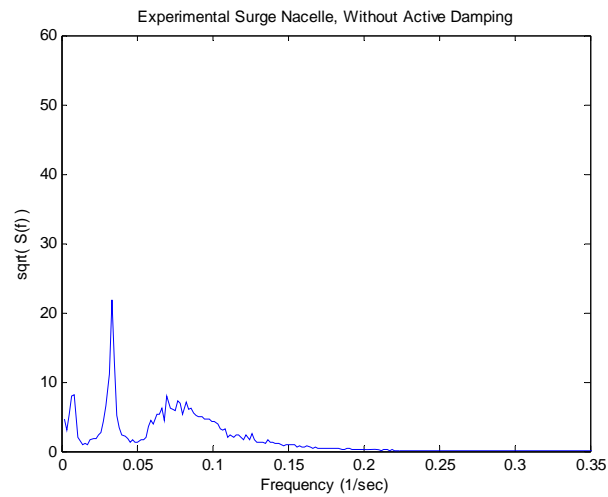


Figure 10. Experiments without active damping. $H_s = 5\text{m}$, $T_p = 12\text{s}$, $U_w = 17\text{ m/s}$

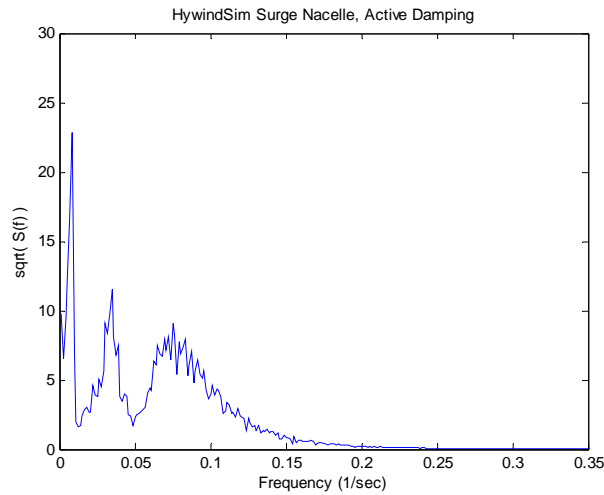


Figure 11. HywindSim simulations with active damping. $H_s = 5\text{ m}$, $T_p = 12\text{ s}$, $U_w = 17\text{ m/s}$.

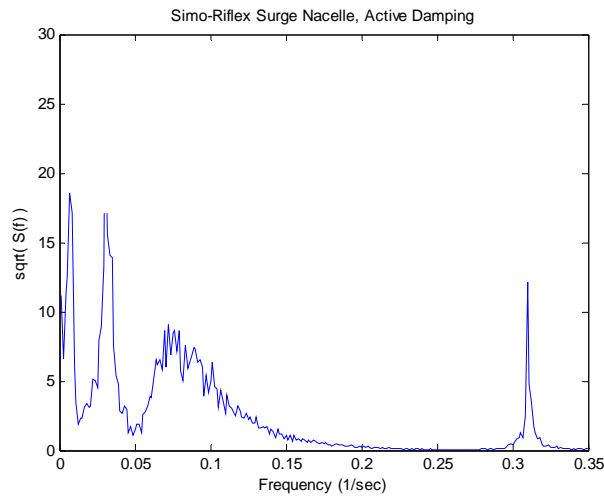


Figure 12. Simo-Riflex simulations with active damping. $H_s = 5\text{ m}$, $T_p = 12\text{ s}$, $U_w = 17\text{ m/s}$.

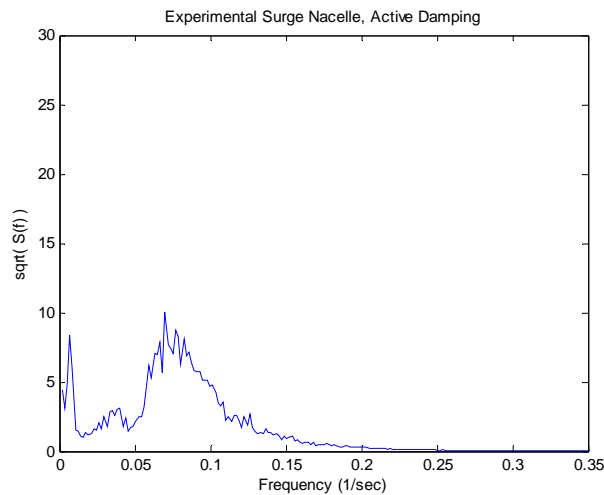


Figure 13. Experiments with active damping. $H_s = 5\text{ m}$, $T_p = 12\text{ s}$, $U_w = 17\text{ m/s}$.

The delay in the build up of lift force on a turbine blade after a sudden change in blade pitch angle is discussed in [12] and illustrated in Figure 14. The results are for the build-up of the lift, ΔL on a two-dimensional foil exposed to a sudden change in circulation, $\Delta\Gamma$. One line is showing the build up of lift on the foil as function of the non-dimensional time, Vt/c , where V is the relative velocity between air and foil, t is time and c is the length of the cord. Results for a single foil as well as an infinite cascade of foils are presented. The infinite cascade may resemble a certain radial section of a

three bladed rotor. In this case we have used a distance between the foils equal to $39.9c$. This is equivalent to the tested turbine at 70% of its full radius. We observe that the interaction effect is sensitive to the tip speed ratio λ . At large tip speed ratios, the build up is faster than for a single foil, but a significant oscillation in the lift force is observed.

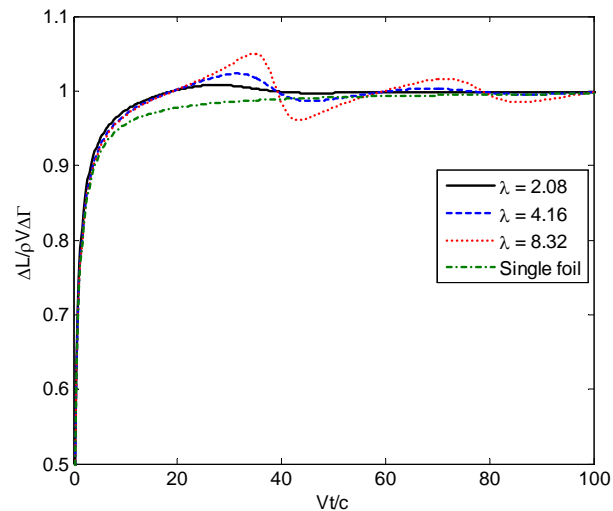


Figure 14. Development of lift force after a sudden change in circulation. Cascade of foils.

5. Discussion and Conclusion

Two different simulation programs have been presented for the Hywind concept for floating offshore wind turbines and a comparative experimental study has confirmed the simulation results.

The experiments have shown that the wave-induced motions are similar as in the simulations. The responses around the natural frequencies are in most cases overestimated by the simulations, and this is an indication of higher damping in the experiments than in the simulations.

A control algorithm for active damping of resonant wind induced tower motions that occur for wind velocities above rated wind speed has shown to be effective both in simulations and model scale experiments.

6. Acknowledgements

MARINTEK is acknowledged for carefully execution of the model tests as well as modification of computational tools. SINTEF Energy Research is acknowledged for their contribution to damping formulation.

7. References

1. Larsen, J.H.M., Soerensen, H.C., Christiansen, E., Naef, S., and Vølund, P. (2005) Experiences from Middelgrunden 40 MW Offshore Wind Farm. COPENHAGEN OFFSHORE WIND 2005, Conference & Exhibition 26-28 October 2005.
2. MacAskill, Alan (2005) DOWNWIND: Marrying Oil and Gas Expertise with Offshore Wind, COPENHAGEN OFFSHORE WIND 2005, Conference & Exhibition 26-28 October 2005
3. Henderson, A.R., 2003. Support structures for floating offshore windfarms, NREL /DOE seminar, Washington, October, 2003.
4. Bulder, B.H., Henderson, A., Huijsmans, R.H.M., Peeringa, J.M., Pierik, J.T.G., Snijders, E.J.B., van Hees, M.Th., Wijnants, G.H., Wolf, M.J.(2003) Floating offshore Wind Turbines for Shallow waters. EWEC 2003, Madrid.
5. Henderson, A.R., Bulder, B., Huijsmans, R., Peeringa, J., Pierik, J. Snijders, E., van Hees, M., Wijnants, G.H. and Wolf, M.J. (2003). Floating windfarms for shallow offshore sites. Proc. Of OWEMES Conference, Naples, Italy.
6. Musial, W., Butterfield, S. and Boone, A., 2004: Feasibility of floating platform systems for wind turbines. National Renewable Energy Laboratory, Golden, CO 80401.
7. Musial, W., Butterfield, S. and Boone, A. (2004). Feasibility of Floating Platform Systems for Wind Turbines. 23rd ASME Wind Energy Symposium, Reno, Nevada, Jan 5-8.
8. Lee, C.-H. and Newman, J.N. (2002). Boundary –Element Methods in offshore Structure Analysis. *OMAE 2001 Conference*, Rio de Janeiro, 2001. Also published in *Journal of Offshore Mechanics and Arctic Engineering*, Vol. 124, pp 81-89 (2002).
9. Haslum, H. and Faltinsen, O.M. (1999). Alternative shape of spar platforms for use in hostile areas. *In Proceedings of Offshore Technology Conference, Paper OTC 10953*, Houston.
10. Fylling, I. J., Larsen, C. M., Sødahl, N., Ormberg, H., Engseth, A., Passano, E. and Holthe, K. (1995). RIFLEX – Theory Manual. SINTEF report no. STF70 F95219.
11. Knauer, A., Hanson, T. D. and Skaare, B., 2006: *Offshore Wind Turbine Loads in Deep-water Environment*. EWEC 2006, Athens.
12. Newman, J.N. (1977) *Marine Hydrodynamics*. MIT Press